Carbohydrate Polymers 92 (2013) 98–105

Contents lists available at SciVerse ScienceDirect

Carbohydrate Polymers

journal homepage: www.elsevier.com/locate/carbpol

Viscoelastic properties and fractal analysis of acid-induced SPI gels at different ionic strength

Chong-hao Bi[a,1], Dong Li[a,1], Li-jun Wang[b,*], Benu Adhikari[c]

[a] College of Engineering, China Agricultural University, P.O. Box 50, 17 Qinghua Donglu, Beijing 100083, China
[b] College of Food Science and Nutritional Engineering, China Agricultural University, Beijing, China
[c] School of Health Sciences, University of Ballarat, VIC 3353, Australia

ARTICLE INFO

Article history:
Received 10 June 2012
Received in revised form 15 August 2012
Accepted 23 August 2012
Available online 30 August 2012

Keywords:
Rheology
Soy protein isolated gel
Confocal laser scanning microscope
Fractal dimension
Scaling model

ABSTRACT

The viscoelastic property and scaling behavior of acid (glucono-δ-lactone)-induced soy protein isolate (SPI) gels were investigated at various ionic strengths (0–800 mM) and five protein concentrations ranging between 4% and 8% (w/w). The infinite storage modulus (G'_∞) and the gelation start time (t_g) which indicate the progress of gelation process exhibited strong ionic strength dependence. The storage modulus and critical strain were found to exhibit a power-law relationship with protein concentration. Rheological analysis and confocal laser scanning microscopy (CLSM) analysis were applied to estimate the fractal dimensions (D_f) of the gels and the values were found to vary between 2.319 and 2.729. The comparison of the rheological methods and the CLSM image analysis method showed that the Shih, Shih, Kim, Liu, and Aksay (1990) model was better suited in estimating the D_f value of acid-induced SPI gel system.

1. Introduction

The control of formation of acid-induced soy protein isolate (SPI) gels for industrial applications calls for a better understanding of the relationship between the microstructure of gels and their macroscopic rheological properties (Ould Eleya, Ko, & Gunasekaran, 2004). The fractal analysis is an effective way to link the microstructure with the macroscopic properties of gels. Fractal structure provides an explanation of the micro-structure of macromolecules (Iannaccone & Khokha, 1996) and is usually applied to describe the complexity of branched molecules (Wang, Li, Wang, Wu, & Özkan, 2011). It can also reflect on the type of the organization of the branches (Wang et al., 2011). The fractal dimension, referred to as D_f, is commonly used to describe the complexity prevailing in gel systems. A number of studies have suggested that the aggregation of protein results into structurally disordered protein particles. These particles show a random mass-fractal on a scale that is far larger than the particle itself (Chodankar, Aswal, Hassan, & Wagh, 2010; Kuhn, Cavallieri, & da Cunha, 2010; Nagano & Tokita, 2011).

To investigate the fractal structure of the gel system and to calculate the value of fractal dimension, scientists have developed a number of methods. These methods can be classified into direct method which is based on confocal laser scanning microscopy, small-angle X-ray scattering, dynamic light scattering; and indirect method which is based on rheological and acoustic properties (Hagiwara, Kumagai, & Nakamura, 1996; Hagiwara, Kumagai, Matsunaga, & Nakamura, 1997; Matsumoto, Kawai, & Masuda, 1992; Wu, Xie, Lattuada, & Morbidelli, 2005).

The rheological tests provide an insight on the microstructure of the gel based on the macromechanical properties that are easy to measure, thus, are commonly applied in fractal analysis. Various scaling models have been developed and used in protein and colloidal gels (Bremer, Bijsterbosch, Schrijvers, & van Vliet, 1990; Mellema, van Vliet, & van Opheudsen, 2002; Shih, Shih, Kim, Liu, & Aksay, 1990; Wu & Morbidelli, 2001). Some models correlate the rheological properties of the gels with the size of gel aggregates, the volume fraction of particles and fractal dimension of the aggregates (Shih et al., 1990; Wu & Morbidelli, 2001).

Among these models, the model developed by Shih et al. (1990) allows the estimation of the fractal dimension solely based on the rheological properties of the gel system. This model calculates the fractal dimension values using storage modulus and critical strain of a gel. This model classifies the gel systems into two regimes: strong-link regime (the intermolecular (or interfloc) links are stronger than the intramolecular or intrafloc links) and weak-link regime (the intermolecular links are weaker than the intramolecular links). Based on the characteristics of a gel (whether it forms strong-link regime or weak-link regime), suitable equation can be chosen to represent or predict the experimental

* Corresponding author. Tel.: +86 10 62737351; fax: +86 10 62737351.
E-mail address: wlj@cau.edu.cn (L.-j. Wang).
[1] These authors contributed equally to this work.

0144-8617/$ – see front matter © 2012 Elsevier Ltd. All rights reserved.
http://dx.doi.org/10.1016/j.carbpol.2012.08.081

Nomenclature

C	SPI concentration (w/w, %)
D	Euclidean dimension (dimensionless)
D_f	fractal dimension (dimensionless)
G'	storage modulus (Pa)
G'_i	initial G' value (Pa)
G'_∞	estimated value of G' at infinite time (Pa)
k	rate empirical parameter (dimensionless)
m	power law exponent (dimensionless)
n	power law exponent (dimensionless)
N_ε	number of boxes at ε scale (dimensionless)
t	time, s
t_g	time when gelation begins (s)
x	fractal dimension of floc backbone (dimensionless)
α	parameter in Wu model (dimensionless)
β	parameter in Wu model (dimensionless)
γ_c	critical strain (%)
ε	corresponding scale (dimensionless)
φ	particle concentration (%)

data. The Shih et al.'s model has been used in soybean globulin, caseinate, β-lactoglobulin, whey protein isolate and flaxseed gum gels (Hagiwara et al., 1997; Pouzot, Nicolai, Durand, & Benyahia, 2004; Wang et al., 2011). The estimated fractal dimension values in these gels were reported to be between 1.41 and 2.82.

Wu and Morbidelli (2001) modified Shih et al.'s model by introducing three parameters α, β and x to define the type of the link in the gel system. Based on the α value, the gels can be classified into three regimes: the strong-link, the weak-link and the transition regimes. Wu and Morbidelli's model was also applied to soybean globulin, bovine serum albumin and flaxseed gum gels (Caillard, Remondetto, & Subirade, 2010; Hagiwara, Kumagai, & Nakamura, 1998; Wang et al., 2011). The estimated fractal dimension values in these gels were reported to be between 1.42 and 2.87.

Acid gelation of SPI is important in food processing industry, such as lactone tofu, and can affect the texture and acceptability of foods. Functional properties of foods such as visco-elasticity and water holding capacity may also get altered during the acid gelation process (Hu, Stanley, Goff, Davidson, & LeMaguer, 1992; Paraskevopoulou & Kiosseoglou, 1997). Soy protein isolate is commonly used as an ingredient in food formulations in order to impart better mechanical properties. The process of making SPI gels involves two steps: heating of soy protein isolate at neutral pH followed by heating of the denatured protein solution at acidic pH after acidification with glucono-δ-lactone (GDL) (Campbell, Gu, Dewar, & Euston, 2009). The ionic strength is known to influence the gel forming characteristics of soy protein isolate (Ikeda, Foegeding, & Hagiwara, 1999; Izumi, Kikuta, Sakai, & Takezawa 1996). Therefore, the microstructure of SPI gels is expected to undergo some changes when the salts are added and the ionic strength (i.e. the salt concentration) is allowed to vary. Commonly, a random aggregation of protein in gels leads to the formation of non-transparent particulate network, especially when subjected to a high ionic strength (Ikeda, Foegeding, & Hagiwara, 1999).

To the best of our knowledge, no research has been undertaken on the fractal structure of acid-induced SPI gels. In this study, the scaling behavior and the fractal dimension of acid-induced SPI gels were investigated using both rheological and the confocal laser scanning microscopy (CLSM) methods. The fractal dimension values obtained from rheological (and associated models) and CLSM image analysis methods were compared. In addition, the effect of ionic strength on the gelling process and the viscoelastic properties of the acid-induced SPI gels were also investigated.

2. Materials and methods

2.1. Materials

Commercial Soy protein isolate (MSZ-90B) (containing 35% of 7S, 52% of 11S) was obtained from Messenger Biotechnology Co. Ltd. (Beijing, China) as a gift. GDL (glucono-δ-lactone) was obtained from Beijing Wohai Technology Ltd. Rhodamine B (BS) was purchased from Beijing Yinghai fine chemical industry. Sodium chloride (AR) was purchased from Beijing Chemical works. All materials are used as supplied.

2.2. Methods

2.2.1. Sample preparation

For rheological tests, the SPI was dissolved in deionized water (pH = 6.7) using a magnetic stirrer (500 r/min) at 25 °C for 20 min in order to prepare 5–8% (w/w) SPI stock solutions. Sodium chloride was then added into the SPI solution to attain ionic strength values between 200 mM and 1000 mM. The stock solutions were then heated at 90 °C for 20 min to fully denature the protein. After cooling to 20 °C, these samples were stored overnight in a refrigerator maintained at 4 °C. For CLSM tests, the stock solutions were also prepared following the same procedure.

2.2.2. Rheological tests

Rheological properties of these acid-induced SPI gels were measured using AR2000ex rheometer (TA Instruments Ltd., Crawley, UK). Aluminum parallel plate (40 mm diameter, 1 mm gap) was chosen to follow the gelling process and measure the gel strength. The temperature was controlled using a peltier unit attached with a water circulation system. GDL (2 g) was added as a powder to 100 ml of stock solution just before the rheological tests. The samples were transferred between parallel plates and the gel was allowed to form in situ at 60 °C. The storage modulus (G') and loss modulus (G'') values were recorded every 30 s during the gel formation process using a constant frequency of 1 Hz and a strain of 1%. A thin layer of silicone oil was applied on the surface of the samples in order to prevent the loss of water due to evaporation. The linear viscoelastic region (LVR) was determined for each sample using strain sweep tests at 1 Hz (data not shown). The viscoelastic properties (G' and G'') of the gels were determined within the LVR.

The end of the gel formation process was considered to be reached when the increase in two consecutive G' values was less than 1%. Once the gelling process was completed, the fully formed gels were subjected to strain sweep measurement, in which the strain was varied from 0.001 to 0.1. The data were recorded at a rate of 20 points per decade. The initial value (G'_i) was calculated as an average value of G'_i at the strain values between 0.001 and 0.01. A critical point was defined as the point at which the G' value reduced to 95% of G'_i (Fig. 1, inset) (Wang et al., 2011). The strain at the critical point was determined and defined as the critical strain (γ_c). The fractal dimensions of the gels were calculated using the G'_i and γ_c.

2.2.3. Confocal laser scanning microscope tests

In all cases, a LEICA TCS SP5 II confocal laser scanning microscope (CLSM) was used to investigate the structural features of acid-induced SPI gels and to determine their fractal parameters. The CLSM was equipped with an inverted microscope (model Leica DMI6000) and He–Ne visible light lasers (Leica Microsystems (CMS) GmbH., Mannheim, Germany). The objective lens used was a 40 × 0.85 HC PL APO lens. Before gelation, the SPI gels were stained with an aqueous solution of Rhodamine B (1 ml of a 0.01% (w/w) Rhodamine B + 10 ml of sample) and then allowed to gel inside a sealed concave slide in a 60 °C water bath for 30 min. The

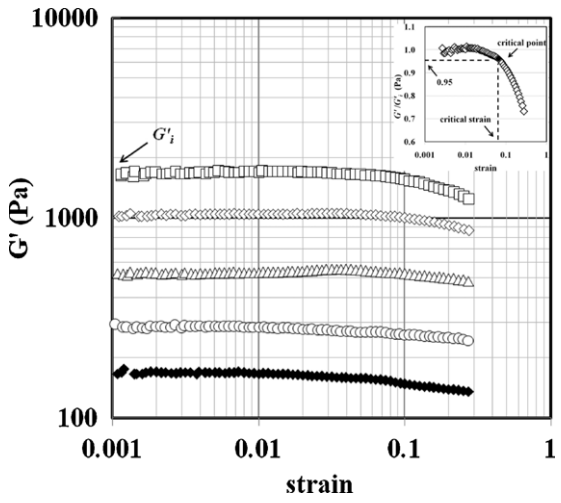

Fig. 1. The storage modulus as a function of strain for the acid-induced SPI gels at various concentrations and ionic strength of 200 mM. G'_i is the estimation of the initial storage modulus. The inset is an illustration for the estimation of the critical point (critical strain).

Rhodamine B was excited at 543 nm with the He–Ne laser and the emission fluorescence was recorded between 561 and 680 nm.

2.3. Theory

2.3.1. Rheological fractal model

The scaling model proposed by Shih et al. (1990) which relates the microscopic structure parameters of colloidal gels to the macroscopic viscoelastic properties are used in this study. Based on the relative strengths of inter- and intra-floc links, two regimes are defined: strong-link regime and weak-link regime (Section 1). The storage modulus of gels (G'_i) and the critical strain (γ_c) are described as proportional to a power of particle concentration (φ).

For a strong-link regime:

$$G'_i \propto \varphi^{(D+x)/(D-D_f)} \tag{1}$$

$$\gamma_c \propto \varphi^{-(1+x)/(D-D_f)} \tag{2}$$

For a weak-link regime:

$$G'_i \propto \varphi^{1/(D-D_f)} \tag{3}$$

$$\gamma_c \propto \varphi^{1/(D-D_f)} \tag{4}$$

where D, D_f and x (where $1 < x < D_f$) are Euclidean, fractal and fractal of floc backbone dimensions, respectively.

Wu and Morbidelli (2001) modified the Shih et al.'s model and introduced a constant (α) (where $0 < \alpha < 1$) in order to evaluate the elastic contribution of both inter- and intra-floc links. It identifies the prevailing regimes in the gelation system and can be an indicator of the relative contribution of the two link types.

$$G'_i \propto \varphi^{\beta/(D-D_f)} \tag{5}$$

$$\gamma_c \propto \varphi^{(D-\beta-1)/(D-D_f)} \tag{6}$$

$$\beta = (D-2) + (2+x)(1-\alpha) \tag{7}$$

where β is an intermediate variable. The notation of all the other parameters is identical to those in Shi et al.'s model.

The volume fraction (φ) of particles in the gels was assumed to be proportional to the SPI concentration (C). Fractal dimension values of SPI gels were calculated using the slope values of log G' versus log C and of log critical strain versus log C, according to the two models (Wang et al., 2011).

2.3.2. Evaluation of fractal dimension (D_f) from CLSM

The microscopic images acquired from CLSM were analyzed using the public domain software ImageJ 1.44p (National Institute of Health, USA). The image micrographs were converted into 8-bit binary images of 1024 × 1024 pixels. The gray level used for thresholding was the median of the gray level histogram of each image. D_f values of the SPI gels were calculated using the box-counting method which is based on the calculation of the scaling rule as follows:

$$D = -\frac{\log\ N_\varepsilon}{\log\ \varepsilon} \tag{8}$$

$$D_f = D + 1 \tag{9}$$

where N_ε is the number of boxes at a certain scale containing part of the image and ε is the corresponding scale. The determination of D_f by image analysis is based on a two-dimensional space. Therefore, when it comes to a three-dimensional space of the gel features, an addition of an extra dimension to the D value is required (Vicsek, 1989).

2.4. Data analysis

The simulation of gelling process and statistical analysis were carried out using SPSS 16.0 (IBM Corporation, USA). The data were subjected to statistical analysis, using one-way analysis of variance (ANOVA) to evaluate the significance of differences and the confidence level was set at 95% ($p < 0.05$).

3. Results and discussion

3.1. Rheological tests

3.1.1. Effect of strain on G'

In order to observe the effect of strain on the G' value, a strain sweep test was conducted on the acid-induced SPI gels (Fig. 1). It can be seen from Fig. 1 that the G' value remains almost constant (plateau) in low strain region. When the strain increases further, and beyond a certain strain value the G' value decreases very sharply indicating a breakdown of bonds in the gel network. This point is also a transition from a linear to a non-linear behavior. As shown in the inset of Fig. 1, when the G' value reached 95% of its initial value (G'_i), the gel system exhibited very fast decline in G' as a function of strain. The strain value at which this transition occurs is called critical strain (γ_c). We have observed that all the samples containing various ionic strengths (200–1000 mM) exhibited similar trend in terms of transition (as seen in Fig. 1) and the presence of critical strain (data not shown).

3.1.2. Effect of ionic strength on G'_∞ and t_g

Fig. 2 shows typical gel formation kinetics of acid-induced SPI in the absence of sodium chloride. When the samples were heated to and maintained at 60 °C, the G' value increased sharply with time and then reached a plateau. The trend of variation of G' with time was similar in other samples having different ionic strength (data not shown). Similar trend of variation of G' with time was reported in the case of other protein gels as well (Ikeda, Foegeding, & Hagiwara, 1999; Ould Eleya et al., 2004).

As the inset in Fig. 2 shows, the trend of increase of G' as a function of time could be fitted to a first-order kinetics model given by Eq. (10).

$$G'(t) = G'_\infty[1 - e^{-k(t-t_g)}] \tag{10}$$

where t is the time (s), t_g is the time (s) at which gelation begins, k is a empirical rate constant (1/s), G'_∞ is the estimated value of G' at infinite time (Pa).

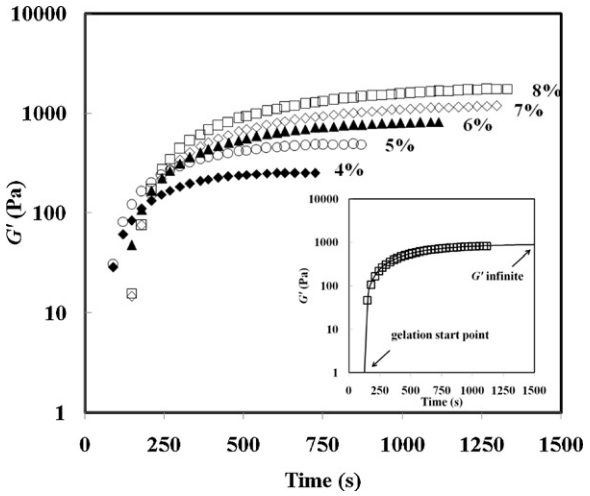

Fig. 2. The gelation profile of the acid-induced SPI gels at various SPI concentrations and at 0 mM ionic strength. The inset shows how the value of G' at considerably long time (G'_∞) and gelation start point (t_g) was determined.

Fig. 3 shows the estimated G'_∞ and t_g values of SPI gels at different ionic strengths. In Fig. 3(a), the G'_∞ value of SPI gel decreases with the increase in the ionic strength and the maximum value of G'_∞ was obtained in the gel which contained no salt. This observation indicates that the gel strength of acid-induced SPI gel becomes weaker with the addition of sodium chloride. This may be due to the fact that electrostatic repulsive forces generated due to the charged protein molecules are very strong and dominant when there is no salt or the salt concentration is very low. When the ionic strength increases, the attractive interactions between molecules become stronger and dominant over repulsive ones. This leads to increased aggregation of the molecules and the gel strength decreases gradually.

Fig. 3(b) shows that when sodium chloride is added, the values of t_g show a slight decrease initially (<200 mM ionic strength) after which it increases sharply (>200 mM ionic strength). This trend suggests that the high ionic strength strongly affects the gelling process and delays the time at which the gelation starts. It can also be observed from Fig. 3(b) that that low ionic strength accelerates the gel formation process in acid-induced SPI gels. The higher t_g values at higher ionic strengths correspond to the trend of G'_∞ at high ionic strength region. The trends in both the G'_∞ and t_g indicate that the addition of salt in high-dose (high ionic strength) increases the difficulty in gel formation process of acid-induced SPI gels.

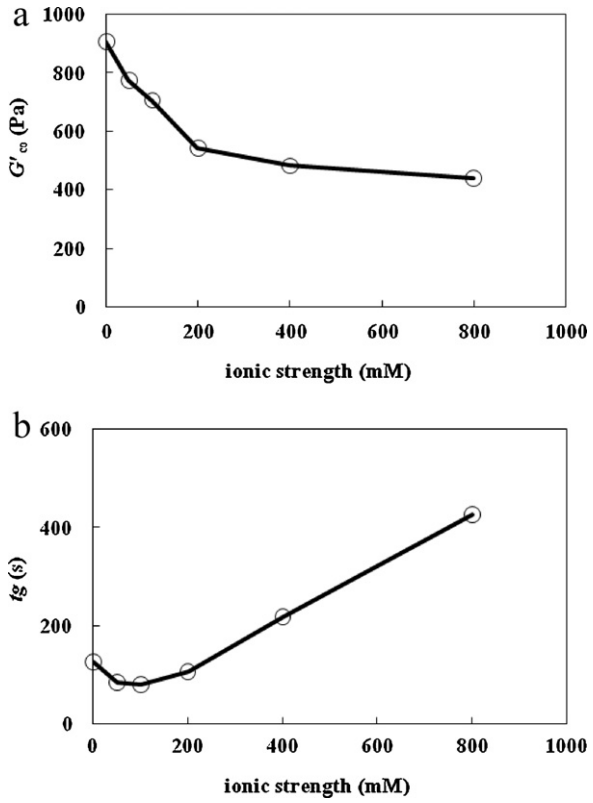

Fig. 3. Effect of the ionic strength on the G' infinite (G'_∞) (a) and gelation start point (t_g) (b) of acid-induced SPI gels at 6% (w/w) of SPI.

3.1.3. Scaling behavior of acid-induced SPI gels

The right hand side of Fig. 4 shows the scaling behavior of critical strain of acid-induced SPI gels as a function of protein concentration. The critical strain γ_c of all the samples shows a power law behavior as a function of SPI concentration, which can be fitted to the form shown by Eq. (11).

$$\gamma_c \propto C^m \tag{11}$$

where m is the power-law exponent. The values of m were found to be strongly influenced by the ionic strength. The maximum and minimum values of this exponent were observed when the ionic strengths were 400 mM (m = 2.829) and 800 mM (m = 0.603), respectively.

Table 1
Effect of the ionic strength on the fractal dimension and evaluated structural parameter of acid-induced SPI gels calculated by CLSM image box-counting method and rheological method (two different models).

Ionic strength (mM)	CLSM image box-counting method	Power-law exponents		Model of Shih et al. (1990)	Model of Wu and Morbidelli (2001)				Regime
	D_f [a]	n [b]	m [c]	D_f [d]	D_f [e]	β [e]	$x=1$ α [e]	$x=1.3$ α [e]	
0	2.631 ± 0.006^A	2.931	2.168	2.66 ± 0.02^A	2.607 ± 0.06^A	1.149	0.950	0.954	Transition
50	2.623 ± 0.003^A	2.896	2.475	2.65 ± 0.04^A	2.627 ± 0.09^A	1.078	0.973	0.976	Transition
100	2.670 ± 0.005^A	2.972	1.082	2.66 ± 0.07^A	2.506 ± 0.08^B	1.466	0.844	0.858	Transition
200	2.729 ± 0.005^A	3.520	2.016	2.72 ± 0.03^A	2.638 ± 0.05^B	1.271	0.909	0.917	Transition
400	2.701 ± 0.004^A	3.539	2.829	2.71 ± 0.06^A	2.685 ± 0.05^A	1.111	0.962	0.966	Transition
800	2.528 ± 0.009^A	2.334	0.603	2.57 ± 0.06^A	2.319 ± 0.11^B	1.589	0.803	0.821	Transition

[A,B] Values in a horizontal (between CLSM, Shih model, and Wu model) with different superscripts were significantly different ($p < 0.05$).
[a] Values of fractal dimensions D_f based on CLSM image box-counting method.
[b] Power law exponent relating G'_i to concentration: $G'_\infty \sim C^n$.
[c] Power law exponent relating γ_c to concentration: $\gamma_c \sim C^m$.
[d] Values of fractal dimensions D_f calculated by the model of Shih et al. (1990).
[e] Values of fractal dimensions D_f, β and α calculated by the model of Wu and Morbidelli (2001).

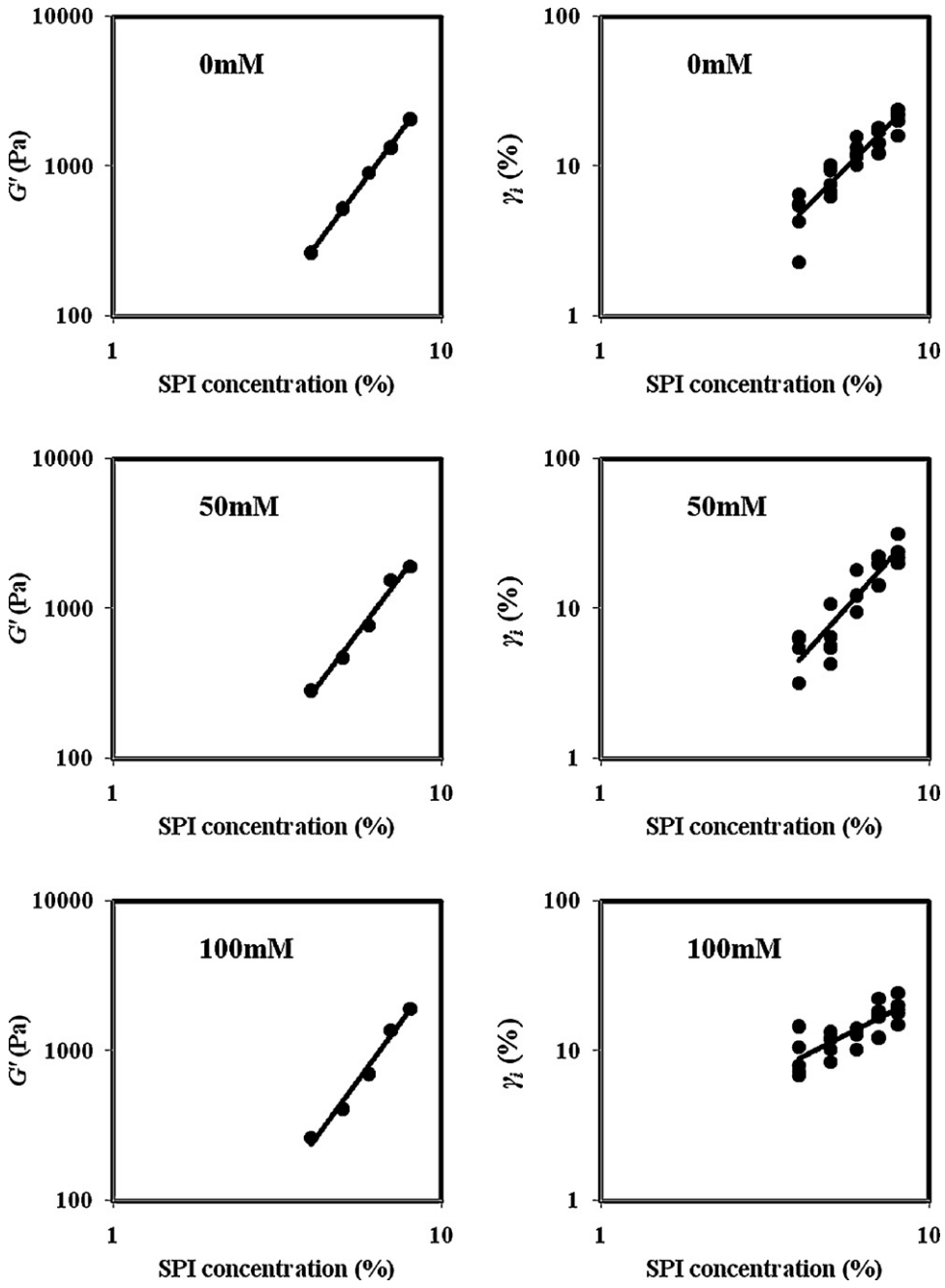

Fig. 4. Effects of concentration and ionic strength on the scaling behavior of the storage modulus (left side) and critical strain of acid-induced SPI gels (right side).

The effect of ionic strength on the scaling behavior of G'_{∞} of SPI gels is shown in the left hand side of Fig. 4. The variation of G'_{∞} values of SPI gels with ionic strength was correlated with the power-law relationship as given by Eq. (12).

$$G'_{\infty} \propto C^{n} \tag{12}$$

where n is the power-law exponent. The n values were also found to be sensitive to the ionic strength; the maximum and minimum values of this exponent were 3.539 and 2.334 at ionic strengths of 400 mM and 800 mM, respectively.

3.1.4. Rheological method of fractal analysis

Table 1 presents the power law exponents (n, m) and D_f values of acid-induced SPI gels at different ionic strengths. All these values were calculated using Shih et al.'s (1990) and Wu and Morbidelli's (2001) models. The m values are positive for all the samples, indicating that the acid-induced SPI gels can be considered as weak-link gel on the basis of Shih et al.'s (1990) model. Eqs. (3) and (4) were applied in order to calculate the values of D_f. The D_f values varied from 2.57 to 2.72, which are very similar to the fractal dimension of β-lactoglobulin, 11S soybean globulin and caseinate gels that were found to vary from 2.6 to 2.7 (Hagiwara et al., 1997).

The fractal dimensions of these gels determined according to Eqs. (5)–(7) based on Wu and Morbidelli's (2001) model are also presented in Table 1. The D_f values calculated from this model were between 2.32 and 2.69 which were lower than the fractal dimension calculated by Shih et al.'s (1990) model. However, fractal dimensions calculated from both the models showed a similar trend regarding the variation of D_f with the increase in the salt concentration. The fact that the Shih et al.'s and Wu and Morbidelli's

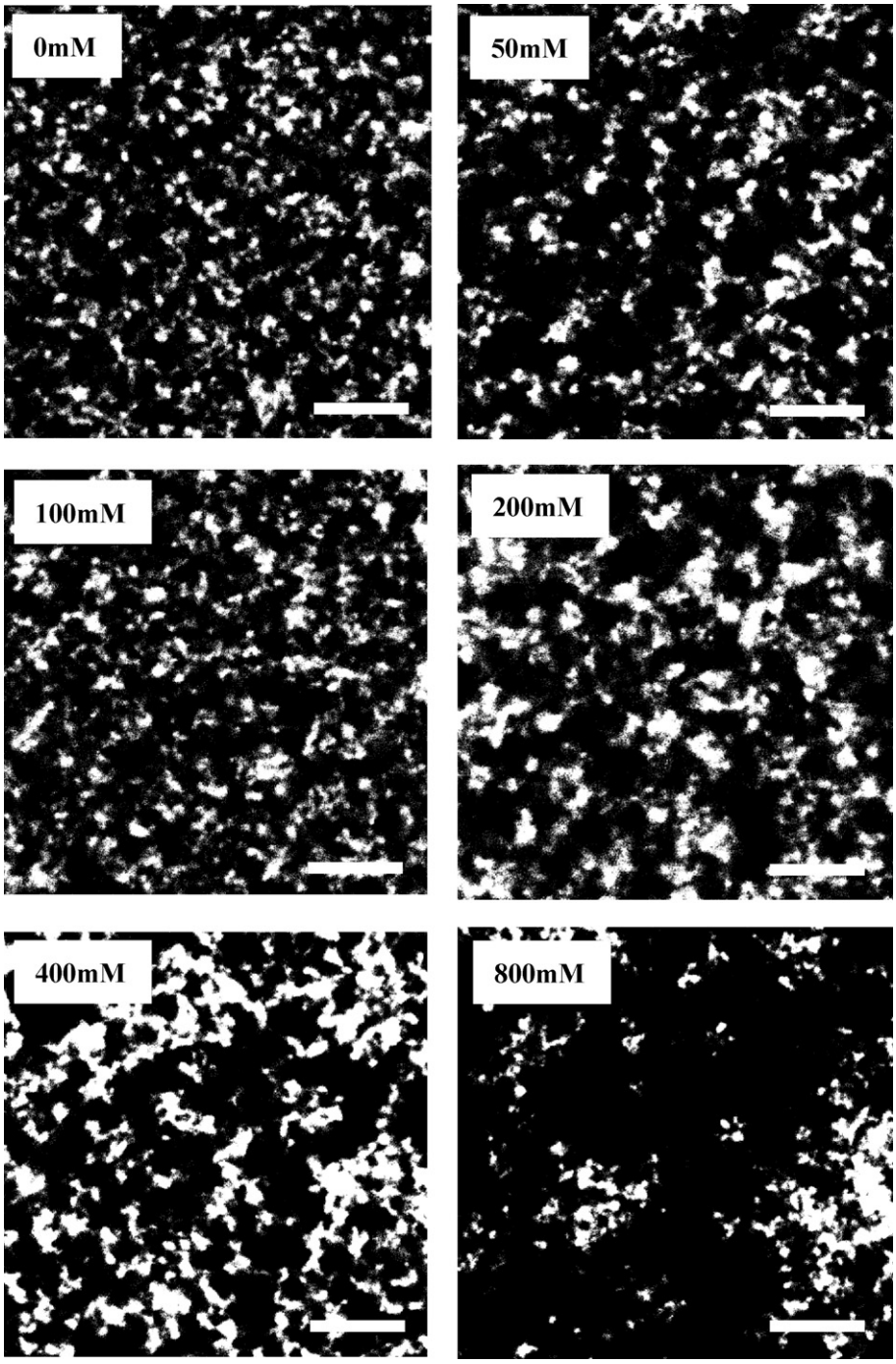

Fig. 5. Micro photographs of SPI gel aggregates at different ionic strength obtained through CLSM. (The bar represents 10 μm.)

models provide different D_f values has also been reported previously in the case of β-lactoglobulin, caseinate and flaxseed gels (Wang et al., 2011; Wu & Morbidelli, 2001).

The Wu and Morbidelli's (2001) model introduces two novel parameters: α and β (Eqs. (5)–(7)). Out of these two parameters, the parameter α distinguishes the type of the gel (strong-link, weak-link or transition gel). This parameter (α) indicates the relative contribution of the inter- and intra-floc links in the network and allows the identification of different gelation regimes dominating the gel system. When $\alpha = 0$, it indicates strong-link; when $\alpha = 1$, it indicates the weak-link; and finally, when $0 < \alpha < 1$, it indicates the transition regime. The parameter α was calculated using two estimated x values ($x = 1$ and 1.3), which are commonly considered to provide good approximation of the fractal dimension of the backbone of colloidal aggregates (Ould Eleya et al., 2004). As can be seen from Table 1 that the α value of all the tested gels varied between 0 and 1, which suggested that all the acid-induced SPI gels can be classified as the transition gels. It has to be noted that all the α values are higher than 0.80, and the gel containing 50 mM concentration of NaCl has α value of 0.98 which is very close to the weak-link regime. This observation explains why these same gels would be classified as the weak-link gels in Shih et al.'s (1990) model.

The results from rheological fractal analysis reveal that the ionic strength affects the fractal dimension of acid-induced SPI gels quite significantly ($p < 0.05$). As it can be seen from Table 1, the highest D_f values of 2.71 (Shih et al.' model) and 2.69 (Wu and Morbidelli's

model) were observed at the ionic strength of 400 mM. The high D_f value indicates a rigid structure of SPI gel aggregate network at 400 mM ionic strength. At 800 mM ionic strength, the lowest D_f values of 2.57 (Shi et al.'s model) and 2.32 (Wu and Morbidelli's model) were observed. The D_f values of acid-induced SPI gels varied between 2.32 and 2.72 when the ionic strength was increased from 0 mM to 800 mM (depending on the choice of the predictive model).

The variation in the ionic strength (salt concentration) affects the structure of the SPI gels and the connection of floc or protein in the gels (i.e. ionic bond). As the D_f values vary with the changes of the gel structure, it gets affected by variation in ionic strength. As the viscoelastic properties of the gels were significantly affected by the ionic strength (Fig. 3a), the fractal structure of acid-induced SPI gels were accordingly affected as a result of the change in ionic strength.

3.2. CLSM method of fractal analysis

The microstructure of the SPI gels observed using CLSM is presented in Fig. 5. These CLSM micrographs show that the microstructure of SPI gels appear homogeneous at most ionic strengths except at 800 mM. These CLSM images further support the fact that the feature of the protein network strongly depends on the ionic strength. The pores within the protein network (the black areas in the images) became larger at high ionic strength and almost completely covered the entire image at 800 mM ionic strength. The increase in the pore size indicates that the strength of protein network is decreasing. The increase in pore size and the subsequent decrease in the protein network strength might have been resulted due to phase separation between protein aggregates and sodium chloride solution. The D_f values of SPI gels in the absence of salt and in the presence of salt at different ionic strength (concentration) can be calculated directly using box-counting method with the images captured from CLSM experiments. The specific procedure of this method was described previously in Section 2.3.2 of this manuscript. Table 1 presents the results of the D_f values calculated from CLSM images. It can be seen from this table that the highest D_f value of 2.729 was obtained from the image when the ionic strength was 200 mM, while the lowest D_f value of 2.528 was obtained at 800 mM ionic strength. The trend of the variation of the D_f values with the varying ionic strength was similar to the D_f values obtained from both the rheological models. It has to be noted that the same numerical values of D_f are sometimes obtained from image analysis even when clear qualitative structural differences are observed visually. Similar observation has been made and reported in other studies (Mellema, Heesakkers, Van Opheusden, & Van Vliet, 2000). This observation suggests that caution has to be exercised while calculating the D_f values of SPI gels through the image analysis method, however, the imaging method gives us important information about the complex extent of the SPI gel network structure.

3.3. Comparison of D_f values obtained from rheological and CLSM methods of fractal analysis

Fig. 6 provides a comparison of the fractal dimensions calculated using the two rheological models and the CLSM image box-counting method. It can be seen from Fig. 6 that the estimated D_f values by rheological analysis varied from 2.32 to 2.72 depending on the model selected and the ionic strength used. We can see from Table 1 that most of D_f values from rheological models were in good agreement ($p < 0.05$) with the D_f values calculated by CLSM image analysis which were between 2.528 and 2.729, especially calculated using Shih et al.'s (1990) model. This agreement indicates that it is feasible to apply the rheological methods in estimating the fractal structure parameter of SPI gels. From Fig. 6, it can be clearly

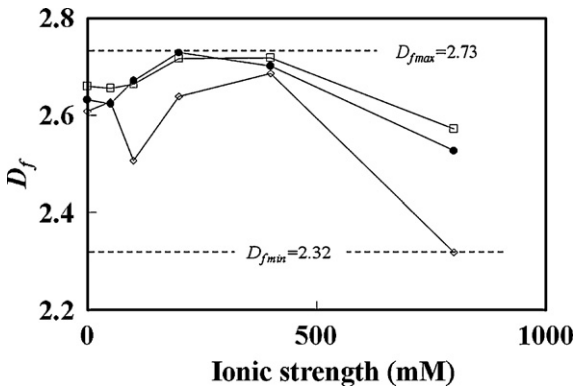

Fig. 6. The comparison of fractal dimensions calculated based on CLSM image analysis (circle dot) and Shih et al. (1990) model (square) and Wu and Morbidelli (2001) (diamond) at different ionic strength.

observed that the fractal dimensions calculated from these two different methods show a similar trend, however, the data from Shih et al.'s (1990) model are closer to the CLSM results. The data presented in Fig. 6 indicates that Shih et al.'s (1990) model is better suited in estimating the fractal dimension of acid-induced SPI gels.

4. Conclusion

The rheological properties and fractal analysis of acid-induced SPI gels were studied as a function of ionic strength (0–800 mM). The result showed that the variation in ionic strength significantly affected the viscoelastic properties of SPI gels. The storage modulus values of the gels were found to decrease with the increase in the ionic strength. Both the storage modulus and the critical strain were found to follow a power law relationship as a function of protein concentration (scaling behavior). Two different fractal models (based on rheological analysis) as well as CLSM based image analysis were applied to calculate the fractal dimension of gels at different ionic strength. And the result showed that it is feasible to apply the rheological methods in estimating the fractal structure parameter of SPI gels, while Shih et al. (1990) model was found to be better suited in estimating the fractal dimension of acid-induced SPI gels. This study provides useful information on gel structure and gel strength of acid-induced SPI gels as quantified by fractal dimension which enables better understanding of the physicochemical properties of acid-induced SPI gels.

Acknowledgement

This research was supported by National Natural Science Foundation of China (31000813).

References

Bremer, L. G. B., Bijsterbosch, B. H., Schrijvers, R., & van Vliet, T. (1990). On the fractal nature of the structure of casein gels. *Colloid and Surfaces*, *51*, 159–170.

Caillard, R., Remondetto, G. E., & Subirade, M. (2010). Rheological investigation of soy protein hydrogels induced by Maillard-type reaction. *Food Hydrocolloids*, *24*(1), 81–87.

Campbell, L. J., Gu, X., Dewar, S. J., & Euston, S. R. (2009). Effects of heat treatment and glucono-δ-lactone-induced acidification on characteristics of soy protein isolate. *Food Hydrocolloids*, *23*, 344–351.

Chodankar, S., Aswal, V. K., Hassan, P. A., & Wagh, A. G. (2010). Effect of pH and protein concentration on rheological and structural behavior of temperature-induced bovine serum albumin gels. *Journal of Macromolecular Science, Part B: Physics*, *49*(4), 658–668.

Hagiwara, T., Kumagai, H., & Nakamura, K. (1996). Fractal analysis of aggregates formed by heating dilute BSA solutions using light scattering methods. *Bioscience, Biotechnology and Biochemistry*, *60*(11), 1757–1763.

Hagiwara, T., Kumagai, H., & Nakamura, K. (1998). Fractal analysis of aggregates in heat-induced BSA gels. *Food Hydrocolloids*, *12*(1), 29–36.

Hagiwara, T., Kumagai, H., Matsunaga, T., & Nakamura, K. (1997). Analysis of aggregate structure in food protein gels with the concept of fractal. *Bioscience, Biotechnology, and Biochemistry*, *61*(10), 1663–1667.

Hu, S. Y., Stanley, D. W., Goff, H. D., Davidson, V. J., & LeMaguer, M. (1992). Hydrocolloid/milk gel formation and properties. *Journal of Food Science*, *57*, 96.

Iannaccone, P. M., & Khokha, M. K. (1996). *Fractal geometry in biological system: An analytical approach*. Boca Roton, FL, USA: CRC Press, Inc., pp. 15–30.

Ikeda, S., Foegeding, E. A., & Hagiwara, T. (1999). Rheological study on the fractal nature of the protein gel structure. *Langmuir*, *15*(25), 8584–8589.

Izumi, Y., Kikuta, N., Sakai, K., & Takezawa, H. (1996). Phase diagrams and molecular structures of sodium-salt-type gellan gum. *Carbohydrate Polymers*, *30*(2–3), 121–127.

Kuhn, K. R., Cavallieri, Â. L. F., & da Cunha, R. L. (2010). Cold-set whey protein gels induced by calcium or sodium salt addition. *International Journal of Food Science and Technology*, *45*(2), 348–357.

Matsumoto, T., Kawai, M., & Masuda, T. (1992). Viscoelastic and SAXS investigation of fractal structure near the gel point in alginate aqueous systems. *Macromolecules*, *25*(20), 5430–5433.

Mellema, M., Heesakkers, J. W. M., Van Opheusden, J. H. J., & Van Vliet, T. (2000). Structure and scaling behavior of aging rennet-induced casein gels examined by confocal microscopy and permeametry. *Langmuir*, *16*(17), 6847–6854.

Mellema, M., van Vliet, T., & Van Opheudsen, J. H. J. (2002). Categorization of rheological scaling models for particle gels applied to casein gels. *Journal of Rheology*, *46*, 11–29.

Nagano, T., & Tokita, M. (2011). Viscoelastic properties and microstructures of 11S globulin and soybean protein isolate gels: Magnesium chloride-induced gels. *Food Hydrocolloids*, *25*(7), 1647–1654.

Ould Eleya, M. M., Ko, S., & Gunasekaran, S. (2004). Scaling and fractal analysis of viscoelastic properties of heat-induced protein gels. *Food Hydrocolloids*, *18*(2), 315–323.

Paraskevopoulou, A., & Kiosseoglou, V. (1997). Texture profile analysis of heat-formed gels and cakes prepared with low cholesterol egg yolk concentrates. *Journal of Food Science*, *6*, 208.

Pouzot, M., Nicolai, T., Durand, D., & Benyahia, L. (2004). Structure factor and elasticity of a heat-set globular protein gel. *Macromolecules*, *37*(2), 614–620.

Shih, W. H., Shih, W. Y., Kim, S. I., Liu, J., & Aksay, I. A. (1990). Scaling behavior of the elastic properties of colloidal gels. *Physics Review A*, *42*, 4772–4779.

Vicsek, T. (1989). Deterministic models of fractal and multifractal growth. *Physica D: Nonlinear Phenomena*, *38*(1–3), 356–361.

Wang, Y., Li, D., Wang, L.-J., Wu, M., & Özkan, N. (2011). Rheological study and fractal analysis of flaxseed gum gels. *Carbohydrate Polymers*, *86*(2), 594–599.

Wu, H., & Morbidelli, M. (2001). A model relating structure of colloidal gels to their elastic properties. *Langmuir*, *17*, 1030–1036.

Wu, H., Xie, J., Lattuada, M., & Morbidelli, M. (2005). Scattering structure factor of colloidal gels characterized by static light scattering, small-angle light scattering, and small-angle neutron scattering measurements. *Langmuir*, *21*(8), 3291–3295.